

High-efficient Isolation of Plant Viral RNA *via* TMAOH-modified Fe₃O₄ Magnetic Nanoparticles

TANG Yan^{1,3}, ZHAO Xiaoli², CHU Linya^{1,4}, SUN Ning^{1,2}, LIU Renxiao¹,
DENG Congliang^{2*} and GE Guanglu^{1*}

1. Key Laboratory of Measurement and Standardization for Nanotechnology of Chinese Academy of Sciences,
National Center for Nanoscience and Technology, Beijing 100190, P. R. China;

2. Beijing Entry-exit Inspection and Quarantine Bureau, Beijing 100026, P. R. China;

3. University of Chinese Academy of Sciences, Beijing 100049, P. R. China;

4. School of Materials Science and Engineering, Shandong University, Jinan 250100, P. R. China

Abstract Magnetic nanoparticles show great potential in RNA enrichment and separation for rapid detection of viral infection. Fundamental studies on the interaction between RNA and nanoparticles with uniform size and surface property are necessary for designing better adsorbent and optimizing the conditions. In this study, monodispersed superparamagnetic magnetite(Fe₃O₄) nanoparticles were synthesized by thermal decomposition and modified with tetramethylammonium hydroxide[N(CH₃)₄OH, TMAOH] that become highly dispersible and stable in water. High-efficiency plant viral RNA adsorption onto TMAOH/Fe₃O₄ nanoparticles in the extracted solution of plant leaves was demonstrated. The changes of surface charge of TMAOH on the Fe₃O₄ nanoparticles with pH contribute to the RNA adsorption and elution. Separating viral RNA with magnetic nanoparticles could be a simple, quick and highly efficient method.

Keywords Magnetic nanoparticle; Fe₃O₄; Tetramethylammonium hydroxide(TMAOH); RNA adsorption

1 Introduction

Magnetic iron oxide nanoparticles are one of the most important nanomaterials because of their unique physicochemical and magnetic properties, which have been widely used in many areas, such as targeted drug delivery^[1], thermal therapy^[2], magnetic resonance imaging(MRI)^[3] and magnetic separation. Among these applications, magnetic separation/isolation is very attractive due to its advantage of convenience and speed over traditional methods such as centrifugation and filtration. The ionic or molecular species to be separated are bound to magnetic particles and isolated from solution in the presence of applied magnetic field. In this regard, nanoparticles with small molecule passivation provide larger contact area, faster diffusion, and larger saturation magnetization per unit mass, and therefore become promising capturing agents^[4]. Recently, magnetic separation *via* nanoparticles has found application in biotechnology and pollution remedy^[5–7].

Nanoparticles have also been used to adsorb and enrich DNA/RNA for biological identification^[8–11]. Telang *et al.*^[10] developed a simple, quick and cheap procedure for DNA extraction from mammal cells using magnetic nanoparticles. Ramanujan *et al.*^[11] studied the magnetic particles coated with polyethylenimine(PEI) to assist gene delivery. While these efforts have demonstrated the effectiveness of nanoparticles to

adsorb and enrich DNA/RNA, a deeper understanding of the interaction between DNA/RNA and magnetic nanoparticle is still desired, to optimize the particle size, surface charge and solution properties for the separation. For nanoparticles, colloidal stability, adsorption capacity, and magnetic response need to be finely tuned and compromised. In addition, previous studies have been mainly focused on DNA adsorption and isolation by magnetic nanoparticles, while the studies of RNA adsorption and isolation by small size magnetite nanoparticles are relatively limited. As for the preparation of magnetic nanoparticles, there have been currently two main schemes of synthesis. One is coprecipitation method^[12,13] that is simple but the obtained nanoparticles easily aggregate and the size distribution of nanoparticles is broad. The other is thermal decomposition method^[14–17] by which one can get monodisperse and highly crystalline nanoparticles, but a hydrocarbon layer usually exists on the nanoparticles. One way of solving this problem is to synthesize Fe₃O₄ nanoparticles *via* a “soft-ligand” route and perform subsequent ligand exchange for phase transfer^[18–20].

We presented the preparation of water-soluble and stable Fe₃O₄ nanoparticles *via* the direct modification of the nanoparticles by tetramethylammonium hydroxide[N(CH₃)₄OH, TMAOH], and demonstrated their effectiveness in viral RNA capture and detection using cucumber green mottle mosaic virus(CGMMV) RNA as an example. The size of Fe₃O₄

*Corresponding authors. E-mail: gegl@nanoctr.cn; dengcl@bjciq.gov.cn

Received June 26, 2013; accepted November 6, 2013.

Supported by the National Basic Research and Development Program of China(No.2011CB932803) and the Special Fund of the General Administration of Quality Supervision, Inspection and Quarantine of the People's Republic of China(No.201110035).

© Jilin University, The Editorial Department of Chemical Research in Chinese Universities and Springer-Verlag GmbH

nanoparticles in this study is among the smallest ones that possess good magnetic response to RNA adsorption compared to previous reports of adsorption.

2 Experimental

2.1 Synthesis of Fe_3O_4 Nanoparticles and TMAOH-modified Fe_3O_4 Nanoparticles

Briefly, 0.5 g of $\text{Fe}(\text{acac})_3$ was dissolved in 20 mL of benzyl alcohol(BA) and then the mixture was heated at a constant heating rate($15\text{ }^\circ\text{C}/\text{min}$) to $190\text{ }^\circ\text{C}$ and stayed at this temperature for 2 h in an air-free environment. After the reaction, we took use of an external magnetic field to collect the black product and wash them with ethanol and hexane. The black product was Fe_3O_4 nanoparticles.

Synthesis of TMAOH/ Fe_3O_4 nanoparticles was performed as follows. The Fe_3O_4 nanoparticles were separated from the reaction solution and washed with ethanol and hexane three times. To 0.005 g of as-prepared Fe_3O_4 nanoparticles was added 5 mL of TMAOH water solution(0.01 mol/L) that was shaken for a few minutes. The TMAOH/ Fe_3O_4 nanoparticles after these treatments were used for further characterization unless otherwise specified.

2.2 Adsorption of RNA from Cucumber Leaves with Fe_3O_4 Nanoparticles and TMAOH/ Fe_3O_4 Nanoparticles

The pretreatment of the samples was as follows. First 50 mg of cucumber leaves infected by CGMMV was ground evenly in the presence of 1 mL of lysis buffer[4 mol/L guanidine thiocyanate, 0.5% sodium *N*-l-auroylsarcosine, 0.1% TritonX-100, 10 mmol/L NaCl, 25 mmol/L sodium citrate ($\text{pH}=5.0$), 2% polyvinyl pyrrolidone(PVP)]. The slurry was transferred to a 1.5 mL microcentrifuge tube that was centrifuged at 5000 r/min for 3 min. Then 50 μL of the supernatant was transferred to a fresh 1.5 mL microcentrifuge tube, to which 50 μL of ethanol and 1 mg of the Fe_3O_4 nanoparticles or TMAOH/ Fe_3O_4 nanoparticles were added. The mixture was vortexed and incubated at room temperature for 5 min, then the suspension was immobilised on a magnetic stand. The supernatant was removed and Fe_3O_4 nanoparticles or TMAOH/ Fe_3O_4 nanoparticles were washed with 70%(volume fraction) ethanol two times, the suspension was immobilised again on a magnetic stand, and the supernatant discarded. Adsorbed RNA was eluted from the Fe_3O_4 nanoparticles or TMAOH/ Fe_3O_4 nanoparticles by addition of 50 μL of TE buffer(10 mmol/L Tris-HCl, 1 mmol/L EDTA, $\text{pH}=8.0$) and incubated with gentle agitation at room temperature for 5 min. The particles were immobilised again, and the eluent was removed and retained.

For RNA quantification, the contents in the supernatants before and after adsorption were determined after precipitation with 2.5 volumes of ethanol and 10% volumes of sodium acetate(0.3 mol/L , $\text{pH}=5.2$). Having been maintained at $-20\text{ }^\circ\text{C}$ for 30 min, the samples were centrifuged at $1.2\times 10^4 g$ for 10 min, washed with 100 μL of 70% ethanol, centrifuged for another 5 min, and resuspended with 50 μL of TE buffer. Purity and

concentration of RNA samples were assessed by UV spectrophotometry at 260 and 280 nm with a Lambda Bio+ (PerkinElmer) spectrometer. Integrity of RNA samples was evaluated on an agarose gel. The RNA samples were diluted to a optimal concentration to detect CGMMV *via* real-time reverse transcription-polymerase chain reaction(RT-PCR).

Real-time RT-PCR assay for the detection of CGMMV was performed as follows. Real-time RT-PCR reactions were set up in 96-well reaction plate *via* one step PrimeScript RT-PCR kit(Takara). All the reactions were carried out in a final volume of 25 μL containing 12.5 μL of 2 \times one step RT-PCR buffer III, 0.5 μL of Takara Ex Taq HS($5\text{ U}/\mu\text{L}$), 0.5 μL of PrimeScript RT Enzyme Mix II, 0.5 μL of forward primer($10\text{ }\mu\text{mol/L}$), 0.5 μL of reverse primer($10\text{ }\mu\text{mol/L}$), 0.3 μL of TaqMan probe($10\text{ }\mu\text{mol/L}$), 1 μL of RNA(10^{-5} — 10^{-9} times dilution), and 9.2 μL of DEPC-water. Thermo-cycling was run on an ABI 7900 nuclein sequence detection system(Applied Biosystems) as follows: 5 min at $42\text{ }^\circ\text{C}$, 10 s at $95\text{ }^\circ\text{C}$, 40 cycles of 5 s at $95\text{ }^\circ\text{C}$, 30 s at $60\text{ }^\circ\text{C}$.

3 Results and Discussion

The average diameter of Fe_3O_4 nanoparticles is about 7 nm from TEM(Fig.S1, see the Electronic Supplementary Material of this paper). From the result of the hydrodynamic size distribution of TMAOH/ Fe_3O_4 nanoparticles(Fig.S2, see the Electronic Supplementary Material of this paper), we can see that the average nanoparticle diameter is 9.5 nm. Compared with the TEM result, this implies that a thin hydration layer exists. Dynamic light scattering(DLS) data further indicate that the Fe_3O_4 nanoparticles in water solution are well dispersed without any significant agglomeration.

From the FTIR spectra of the unpassivated Fe_3O_4 nanoparticles(Fig.1 curve *a*) and TMAOH/ Fe_3O_4 nanoparticles (Fig.1 curve *b*), an intense and broad band appears nearby 3421 cm^{-1} corresponding to the O—H stretching vibration. This indicates that the surfaces of Fe_3O_4 nanoparticles are readily covered with hydroxyl group in the aqueous environment. Moreover, C—H(CH_2) asymmetrical and symmetrical stretching at 2909 and 2845 cm^{-1} appear in Fig.1 curve *a* while disappear in Fig.1 curve *b*, meaning that the benzyl alcohol as a weak ligand has been replaced by TMAOH. Another vibrational feature at 1132 cm^{-1} is assigned to the C—N stretching mode. The COO^- asymmetrical and symmetrical stretching are

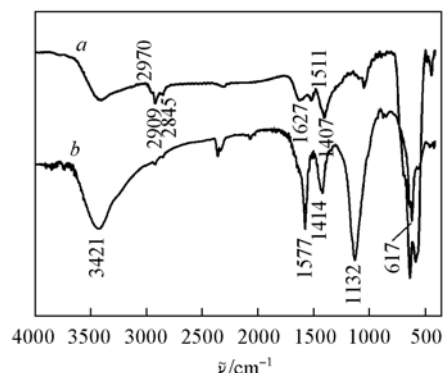


Fig.1 FTIR spectra of Fe_3O_4 nanoparticles(*a*) and TMAOH/ Fe_3O_4 nanoparticles(*b*)

around 1511 and 1407 cm^{-1} respectively, and the C=O stretching is around 1627 cm^{-1} (Fig.1 curve a)^[21]. The results were caused by the coordination effect of benzoic acid which was from the oxidization of benzyl alcohol^[22]. In Fig.1 curve b, these peaks migrate rather than disappear which means the coordination between COO^- and Fe atom is strong chemical interaction that cannot be replaced by TMAOH, but the interaction can be influenced by TMAOH on the surface of nanoparticles. All these characteristic peaks indicate the adsorption of TMAOH on the Fe_3O_4 nanoparticles.

ζ -Potential of the nanoparticles not only reflects the charging of the surface modified molecule, but also helps to understand the adsorption behavior in this system. According to this, we can design some adsorbents with the help of the electrostatic force or optimize the conditions to better serve the purpose of adsorption.

The ζ -potential of TMAOH/ Fe_3O_4 nanoparticles which were dispersed in water solution *vs.* different pH values is plotted in Fig.2. The nanoparticles keep negatively charged in the pH range from 9 to 13 and keep positively charged below pH=5. For the pH range from 5 to 9, the solution cannot exist stably, because there are not enough charges on the nanoparticle's surface. When we took the RNA adsorption process, the pH of the solution was chosen around 5, while the charges of nanoparticles were positive, which contributed to RNA adsorption by electrostatic attraction.

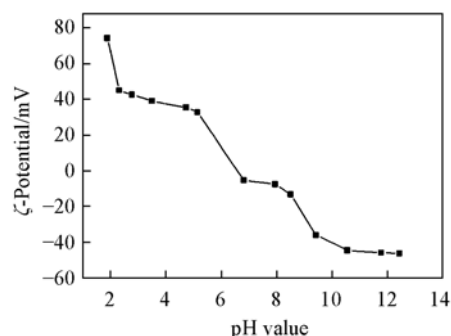


Fig.2 ζ -Potential of TMAOH/ Fe_3O_4 nanoparticles in aqueous solution at different pH values

In addition, we measured the ζ -potential of the TMAOH/ Fe_3O_4 nanoparticles in solutions with different TMAOH concentrations and the NaCl solution of different ionic strengths (Fig.S3, see the Electronic Supplementary Material of this paper). These results imply that this water-soluble TMAOH/ Fe_3O_4 nanoparticles system could suffer itself to a large concentration range and a certain ionic strength.

We also measured the saturation magnetization of the Fe_3O_4 nanoparticles before and after modified. We have found that there is little change in it. The difference is negligible because both are around 5×10^4 A/m (Fig.S4, see the Electronic Supplementary Material of this paper). In the solution, the nanoparticles show apparent movement towards the magnetic field, which should be useful for future enrichment, separation and detection applications, such as RNA/DNA adsorption and detection.

In this research, a plant viral RNA is chosen for adsorption. Cucumber green mottle mosaic virus (CGMMV) is a member of

the genus tobamovirus infecting cucurbit plants. This virus is seed-transmitted that can be easily transmitted mechanically. CGMMV is an alien invasive pathogen^[23] and it remains a potential serious threat to the production of cucurbitaceous crops. In May, 2007, CGMMV was listed as a quarantine pest in China. And a rapid, reliable and sensitive detection method is very important for the prevention and control of the disease caused by CGMMV.

Using Fe_3O_4 nanoparticles and TMAOH/ Fe_3O_4 nanoparticles, we successfully absorbed RNA from cucumber leaves infected by CGMMV (Fig.3). RNA samples showed intact 28S and 18S rRNA bands on agarose gel. The concentrations, recovery yields and $A_{260/280}$ ratios of RNA samples adsorbed with Fe_3O_4 or TMAOH- Fe_3O_4 were determined. The data obtained are presented in Table 1.

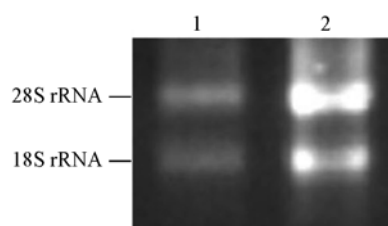


Fig.3 Agarose gel electrophoresis of RNA samples isolated with Fe_3O_4 nanoparticles (lane 1) and TMAOH/ Fe_3O_4 nanoparticles (lane 2)

Table 1 Viral RNA adsorption by Fe_3O_4 nanoparticles and TMAOH/ Fe_3O_4 nanoparticles

Nanoparticle	Supernatant	A_{260}/A_{280}	Concentration/ ($\text{ng} \cdot \mu\text{L}^{-1}$)	Yield(%)
Fe_3O_4	Before adsorption	1.967	209.8	—
	After adsorption	1.117	2.0	32
	Eluent	1.972	66.4	—
TMAOH- Fe_3O_4	Before adsorption	1.967	209.8	—
	After adsorption	1.333	2.5	93
	Eluent	2	195.1	—

Spectrophotometer analysis reveals that the $A_{260/280}$ ratios of eluted RNA samples ranged from 1.9 to 2.0, indicating that the RNA adsorption by Fe_3O_4 or TMAOH- Fe_3O_4 was largely free of contaminating proteins. UV spectroscopic analysis reveals that the recovery yield of RNA adsorbed by TMAOH/ Fe_3O_4 nanoparticles is higher than that of Fe_3O_4 nanoparticles. It is shown that RNA containing phosphate groups has strong interaction with Fe_3O_4 nanoparticles^[24–26]. When the Fe_3O_4 nanoparticles are used to adsorb RNA, strong interactions between the phosphate group of RNA and the Fe_3O_4 nanoparticle make it difficult to elute RNA, which results in a reduction in recovery of RNA. However, the Fe_3O_4 nanoparticles modified by TMAOH are a better adsorbent for RNA because the yield of RNA recovered is significantly high. This is due to the double electrode layer of TMAOH/ Fe_3O_4 nanoparticles which could prevent RNA from binding the Fe_3O_4 nanoparticles directly.

Table 2 shows the sensitivity of CGMMV detection by real-time RT-PCR. The highest dilution at which the real-time RT-PCR assay could still detect CGMMV was 10^{-9} with an average cycle threshold (CT) value of 36.61 ± 0.27 , under which the CGMMV RNA was absorbed *via* TMAOH/ Fe_3O_4

nanoparticles. CGMMV could still be detected by real-time RT-PCR assay under the highest dilution of RNA at 10^{-8} , under which the RNA was absorbed *via* Fe_3O_4 nanoparticles. In addition, the CT value of each 10-fold-diluted CGMMV RNA (from 10^{-5} to 10^{-9}) adsorbed by TMAOH/ Fe_3O_4 nanoparticles is smaller (approximately 2.42 cycles) than that by Fe_3O_4 nanoparticles.

Table 2 Real-time RT-PCR detection of CGMMV RNA absorbed by Fe_3O_4 nanoparticles and TMAOH/ Fe_3O_4 nanoparticles*

Dilution gradient	CT value \pm SD	
	Fe_3O_4 nanoparticles	TMAOH/ Fe_3O_4 nanoparticles
10^{-5}	25.87 \pm 0.05	23.07 \pm 0.09
10^{-6}	28.50 \pm 0.29	26.36 \pm 0.15
10^{-7}	31.49 \pm 0.14	29.35 \pm 0.15
10^{-8}	34.96 \pm 0.31	32.31 \pm 0.26
10^{-9}	—	36.61 \pm 0.27

* CT: Cycle threshold value and the CT values for each dilution are the means of three replicates; SD: standard deviation. CT values of greater than 38 cycles were considered negative.

The results indicate that the adsorption method of RNA by TMAOH/ Fe_3O_4 nanoparticles is efficient, inexpensive, and highly reproducible. And this method can be combined with real-time RT-PCR to detect plant virus. In addition, TMAOH/ Fe_3O_4 nanoparticles have been successfully applied to the detection of Arabis mosaic virus (ArMV) and Lily symptomless virus (LSV). According to the results, a scheme about the Fe_3O_4 nanoparticles modified by TMAOH (Fig.S5, see the Electronic Supplementary Material of this paper) is given.

4 Conclusions

A two-step method combining high-temperature organo-metallic synthesis with modification by tetramethylammonium hydroxide (TMAOH) has been developed to prepare highly water-dispersible Fe_3O_4 nanoparticles with narrow size distribution, which show applicable response to magnetic field. And the effect of adsorption of nucleic acid is better when the Fe_3O_4 nanoparticles are modified by TMAOH. So this nanoparticle system could be useful for detecting viruses.

Electronic Supplementary Material

Supplementary material is available in the online version of this article at <http://dx.doi.org/10.1007/s40242-014-3269-x>.

References

- [1] Hao R., Xing R. J., Xu Z. C., Hou Y. L., Gao S., Sun S. H., *Adv. Mater.*, **2010**, 22, 2729
- [2] Qu J. M., Liu G., Wang Y. M., Hong R. Y., *Adv. Powder Technol.*, **2012**, 21, 461
- [3] Jun Y. W., Huh Y. M., Choi J. S., Lee J. H., Song H. T., Kim S., Yoon S., Kim K. S., Shin J. S., Suh J. S., Cheon J., *J. Am. Chem. Soc.*, **2005**, 127, 5732
- [4] Pan Y., Du X. W., Zhao F., Xu B., *Chem. Soc. Rev.*, **2012**, 41, 2912
- [5] Wang L., Yang Z. M., Gao J. H., Xu K. M., Gu H. W., Zhang B., Zhang X. X., Xu B., *J. Am. Chem. Soc.*, **2006**, 128, 13358
- [6] Jin Y. J., Liu F., Tong M. P., Hou Y. L., *J. Hazard. Mater.*, **2012**, 227/228, 461
- [7] Cha D. M., Han Z. H., Ma T., Li B. H., Liu G. Q., Zhu W., *Chem. J. Chinese Universities*, **2013**, 34(4), 760
- [8] Jiang H. H., Han X. Y., Li Z. L., Chen X. C., Hou Y. H., Gai L. G., Li D. C., Lu X. R., Fu T. L., *Colloids and Surface A: Physicochem. Eng. Aspects*, **2012**, 401, 74
- [9] Chiang C. L., Sung C. S., Chen C. Y., *J. Magn. Magn. Mater.*, **2006**, 305, 483
- [10] Saiyed Z. M., Bochiwal C., Gorasia H., Telang S. D., Ramchand C. N., *Anal. Biochem.*, **2006**, 356, 306
- [11] Ang D., Nguyen Q. V., Kayal S., Preiser P. R., Rawat R. S., Ramamujan R. V., *Acta. Biomater.*, **2011**, 7, 1319
- [12] Kang Y. S., Risbud S., Rabolt J. F., Stroeve P., *Chem. Mater.*, **1996**, 8, 2209
- [13] Jolivet J. P., Chaneac C., Tronc E., *Chem. Comm.*, **2004**, 481
- [14] Sun S. H., Zeng H., *J. Am. Chem. Soc.*, **2002**, 124, 8204
- [15] Sun S. H., Zeng H., Robinson D. B., Raoux S., Rice P. M., Wang S. X., Li G. X., *J. Am. Chem. Soc.*, **2004**, 124, 273
- [16] Park K. J., An Y. S., Hwang Y. S., Park J. G., Noh H. J., Kim J. Y., Park J. H., Hwang N. M., Hyeon T., *Nat. Mater.*, **2004**, 3, 891
- [17] Park J., Lee E., Hwang N. M., Kang M. S., Kim S. C., Hwang Y., Park J. G., Noh H. J., Kini J. Y., Park J. H., Hyeon T., *Angew. Chem. Int. Edit.*, **2005**, 44, 2872
- [18] Pinna N., Grancharov S., Beato P., Antonietti M., Niederberger M., *Chem. Mater.*, **2005**, 17, 3044
- [19] Liu B. J., Li X. Y., Chen W., Liu R. X., Ge G. L., *Acta Phys.-Chim. Sin.*, **2010**, 26, 784
- [20] Li X. Y., Tang Y., Ge G. L., *Sci. China Phys. Mech. Astron.*, **2011**, 54, 1766
- [21] Taniguchi T., Nakagawa K., Watanabe T., Matsushita N., Yoshimura M., *J. Phys. Chem. C*, **2009**, 113, 839
- [22] Zhou S. X., Garnweitner G., Niederberger M., Antonietti M., *Langmuir*, **2007**, 23, 9178
- [23] Chen J., Li M. F., *Plant Quarantine*, **2007**, 2, 94
- [24] Taylor J. I., Hurst C. D., Davies M. J., Sachsinger N., Bruce L. J., *J. Chromatogr. A*, **2000**, 890, 159
- [25] Daou T. J., Begin-Colin S., Grenèche J. M., Thomas F., Derory A., Bernhardt P., Legare P., Pourroy G., *Chem. Mater.*, **2007**, 19, 4494
- [26] Sahoo Y., Pizem H., Fried T., Golodnitsky D., Burstein L., Sukenik C. N., Markovich G., *Langmuir*, **2001**, 17, 7907